Study of the effect of exciton annihilation lifetime on some kinematic and intrinsic parameters of a silicon heterojunction solar cell (HIT), illuminated by monochromatic light

Abstract

In this article, with a view to improving the efficiency of photovoltaic cells, and given the promising yields of silicon heterojunction photovoltaic cells, we have, using a silicon heterojunction cell (a-Si:H/c-Si) doped with (n^+p), studied the contribution of excitons to the internal quantum efficiency of charge carriers.

We then developed a detailed explanation of the energy conversion phenomena, based on an exciton-exciton annihilation process, which allows the electrons of quasiparticles to retain some of their energy. We used a numerical method for solving the charge carrier transport equations and carried out some additional calculations, which enabled us to obtain some results.

These results then enabled us to study the influence of the annihilation lifetime on the charge carrier photo-current density, leading to internal charge carrier quantum yields of between 29.29768% and 77.8525%.

Keywords: Photovoltaic system, Electricity grid, Self-consumption, Self-generation, Expense, profitability.

1. Introduction

The effect of excitons in a solar cell has long been considered unimportant for the production of photovoltaic energy by some researchers. Until recently, the effect of excitons on current transport has not been studied because excitons are neutral and their number in semiconductors at a temperature greater than or equal ambient temperature has been considered insignificant [1]. This view was modified by Hangleiter [2], who highlighted the role of excitons in recombination via deep impurities [3] and improved Auger-band recombination by electron-hole correlation [4]. This theory has been confirmed experimentally by many authors [2,5,6].

But despite all these advances, excitonic theories are complex and often difficult to solve analytically. This led some authors like [7] to use a numerical resolution method. Others like [8,9,10], based on quantum phenomena, studied the annihilation of excitons in a semiconductor.

As a continuation of all this work, we used the annihilation life of excitons in a silicon heterojunction cell (HIT) to understand its influence on the kinematic and intrinsic parameters of the HIT cell.

2. Exciton-exciton annihilation:

Annihilation can be defined as a transition between two excited states by a transfer of energy [11]. Energy transfer occurs not only between a donor (in an excited state) and an acceptor (in the ground

state) [12,13,14,15]. But transitions between two excited states (an excited donor and an excited acceptor) can also occur, resulting in a donor with higher energy levels and an acceptor with a lower excited state or an acceptor in the ground state. This process of energy transfer between two excitons is known as exciton annihilation [16,17,18]. Exciton annihilation becomes increasingly important when the excitation density is high. Since the excitons in inorganic semiconductors (silicon) are of the Wannier type [19,20,21], it is more correct to study the time at which excitons annihilate than to study their lifetime, since annihilation does not directly recombine excitons [22,23,24], but destroys their excited states, which allows them to transit to higher states or relax to excitonic states lower in energy [25,26,27]. In this case, the exciton's diffusion length corresponds to the distance travelled in matter before its annihilation. This length is limited by the finite lifetime of the exciton (the exciton lifetime) in a defect-free material.

The phenomenon of annihilation by energy transfer between two excitons can lead to the emission of one, two or more photons or simply to a release of heat. When two excitons annihilate, one of the excitons (donor) gives up part of its energy to the other exciton (acceptor) by relaxing to a lower energy level and allowing the acceptor to transit to a higher energy exciton level before relaxing and losing its energy in the form of heat. Contrary to direct recombination where the two excitons recombine while losing their energies or to the intra-band relaxation which leads to two excitons which are at a lower excitonic level, the exciton-exciton annihilation delays the recombination of the excitons and allows them to diffuse as long as possible in the photovoltaic cell (see figure 1 and 2).

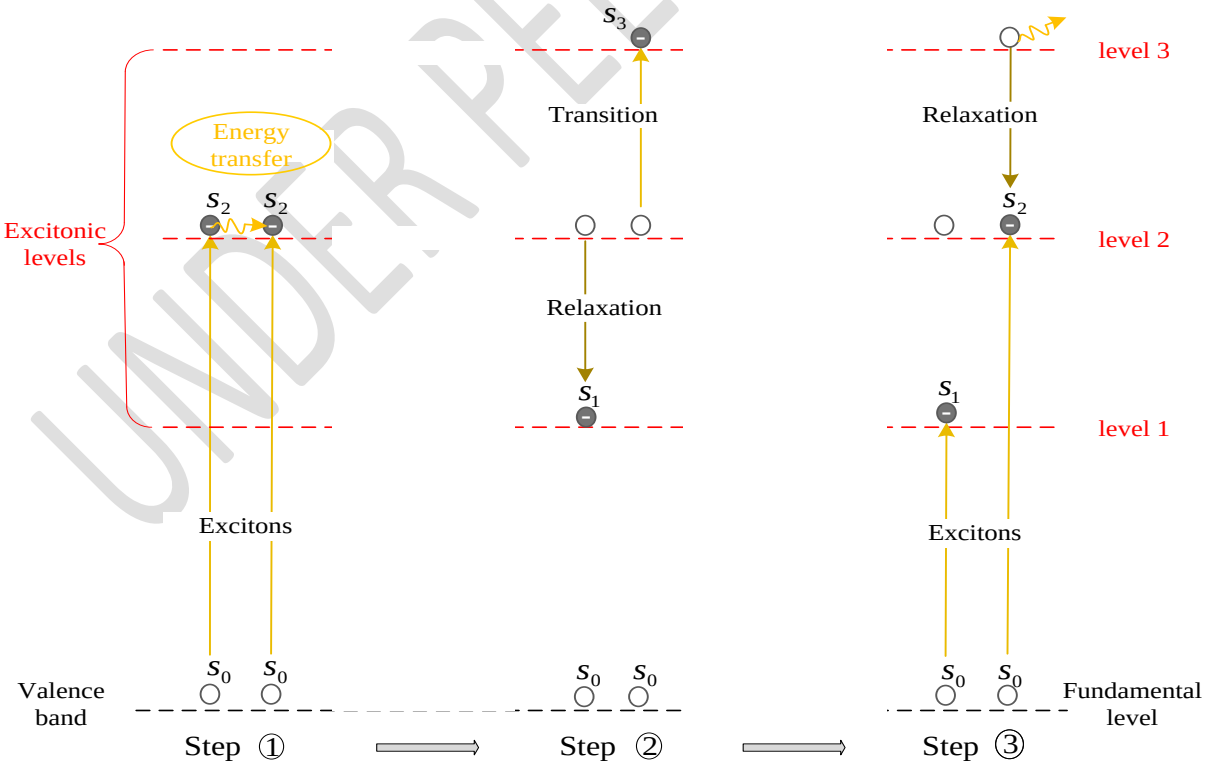

Figure 1: Internal conversion of the excitation energy of an electron of the second excitonic level by an exciton-exciton annihilation process

The annihilation process of two excitons which are at the second excitonic level is described by 3 steps defined as follows :

- the energy transfer between the donor singlet exciton and the acceptor singlet exciton at the second excitonic level ;
- the transition of the singlet acceptor exciton to the third excitonic level and the relaxation of the singlet donor exciton to the first excitonic level ;
- a relaxation of the singlet acceptor exciton from the third excitonic level to the second excitonic level by losing part of its energy in the form of heat.

We have noticed that two excitons of the level 2 by annihilating each other change excitonic state, but do not recombine. Since in our study the excitons are in the Wannier state, then the annihilation changes the Wannier state of the excitons. This results in an unstable singlet exciton of the first excitonic level and an unstable singlet exciton of the second excitonic level. Thus, this physical phenomenon can be described as a change of physical state:

$$S_2 + S_2 \rightarrow S_1 + S_3^* \rightarrow S_1 + S_2 + \text{heat}$$

S denotes the type of exciton (Singlet exciton), the subscripts 1,2,3 represent the 1,2,3 excitonic energy levels, respectively, and the star (*) defines a highly unstable excitonic state.

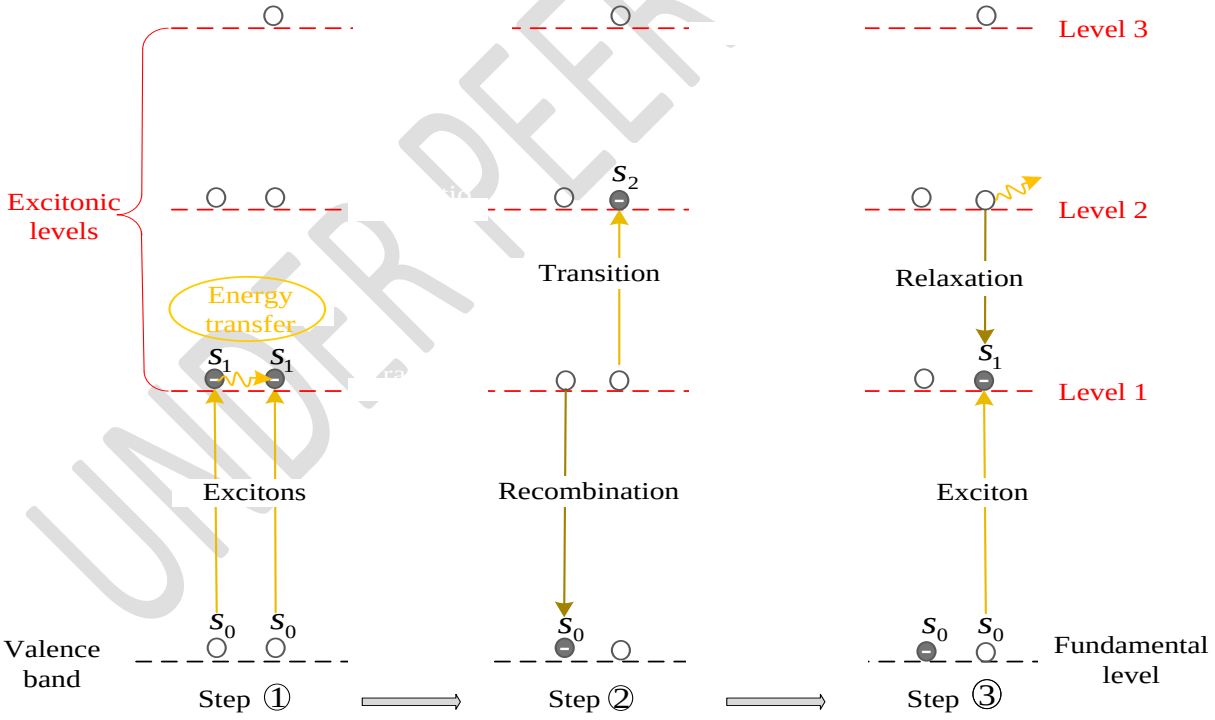

Figure 2: Internal conversion of the excitation energy of an electron of the first exciton level by an exciton-exciton annihilation process

In the case of the annihilation of two singlet excitons of level 1, we observe the same steps and processes of annihilation of two singlet excitons of level 2, but with different results.

- First an energy transfer between the donor singlet exciton and the acceptor singlet exciton at level 1.

- Then a transition of the singlet acceptor exciton to level 2 and a relaxation of the singlet donor exciton to the fundamental level.
- Finally a relaxation of the singlet exciton acceptor from level 2 to level 1 by losing part of its energy in the form of heat.

The result is a stable electron in the fundamental state and an unstable singlet exciton in level 1. Thus, this physical phenomenon can be described by the following change of physical state:

$$S_1 + S_1 \rightarrow S_0 + S_2^* \rightarrow S_0 + S_1 + \text{heat}$$

S_0 is a stable singlet state while S_1 and S_2 are unstable excited singlet states or simply singlet excitons. This reaction can be generalized with excitons in any excitonic energy level.

$$S_n + S_n \rightarrow S_{n-1} + S_{n+1}^* \rightarrow S_{n-1} + S_n + \text{heat}$$

With n representing the nth excitonic energy level. The process can stop at the second step of annihilation and the acceptor exciton which is in a very unstable state can be collected before relaxing. Let us recall that this is only one possibility among others. We cannot study all the physical phenomena that govern the annihilation between two or more excitons of the same type (singlet-singlet) or of different types (singlet-triplet) [28,29]. And knowing that one can have several excited levels (n) where excitons can annihilate, one can only note the unpredictable character of excitons. Moreover, the relaxation phenomena described in [30], combined with the annihilation of excitons and the short lifetime of excitons, make the study of excitonic phenomena in semiconductors complex. The fact that excitons are very much in the minority compared to free charge carriers causes most researchers to neglect them in their papers [31,32,33]. While authors like M. Faye [34], S. Zh. Karazhanov [35], R. Corkish [36] and so many other researchers concerned with the importance of excitons in photovoltaic cells, have proved in one way or another their contribution to photovoltaic energy production.

At present, it would not be possible to theoretically describe excitonic phenomena in the most reliable or explicit way, without resorting to quantum mechanics. More precisely, exciton annihilation is often described by quantum mechanics with the annihilation operator which defines the Wannier state change of the exciton or "destroys the exciton". This operator is always accompanied by the creation operator which describes the ability of excitons to move in the crystal lattice from one to the other and the interactions between the two operators which define the excitonic nature of the particles see [29,37,38]. Moreover, when the electrons of a crystal are pushed into interstitial positions, we say that the excitons annihilate, in a delocalized state.

3. Modeling:

We consider a silicon heterojunction cell of type (n^+p), length L, illuminated by monochromatic light in the presence of excitons.

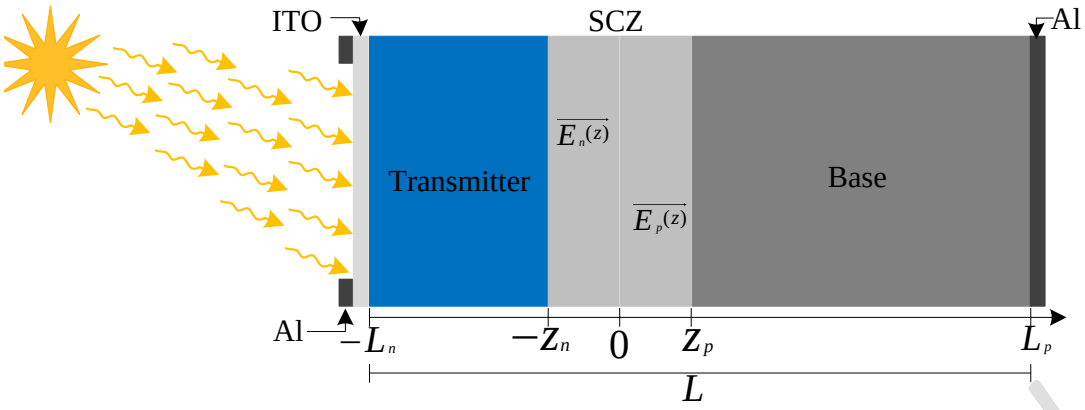

Figure 3: Structure of a silicon heterojunction solar cell (a-Si:H/c-Si), type (n^+p)

The cell is composed of three parts:

- The emitter: area heavily doped with donor atoms 10^{19} cm^{-3} ;
- The space charge zone (SCZ): located between the emitter and the base where an electric field prevails. This field allows the separation of electron-hole pairs that arrive at the junction ;
- The base: quasi-neutral zone, doped with acceptor atoms $1.14x10^{17}$ cm^{-3}.

The mechanisms of generation, recombination and diffusion govern the continuity equations.

3.1 Transport of charge carriers in the base

In the (p)-type doped base, the minority carriers, which are electrons with charge (-q), come from free electron-hole pairs and excitons. The density of free or bound electrons obeys the law of charge conservation. We describe the photogeneration transport of minority electrons in the base (n_e) and electrons from bound electron-hole pairs: excitons (n_x), by the system of differential equations (1).

$$\begin{cases} D_e \dfrac{\partial^2 n_e}{\partial z^2} + m_e \dfrac{\partial [n_e E_p(z)]}{\partial z} = \dfrac{n_e - n_{e0}}{t_e} + b.N_A(n_e - n_{e0}) - \dfrac{n_x - n_{x0}}{t_d} - G_e \\ D_x \dfrac{\partial^2 n_x}{\partial z^2} + m_x \dfrac{\partial [n_x E_p(z)]}{\partial z} = \dfrac{n_x - n_{x0}}{t_a} - b.N_A(n_e - n_{e0}) + \dfrac{n_x - n_{x0}}{t_d} - G_x \end{cases} \quad (1)$$

Where (D_e) and (D_x) are the scattering coefficients of electrons from free electron-hole pairs and excitons, b is the volume coupling coefficient of bound electron and hole, (n_{e0}) and (n_{x0}) their equilibrium concentrations, (N_A) is the concentration of acceptors in the base, τ_a is the exciton annihilation lifetime, τ_e the electron lifetime, τ_d the exciton dissociation lifetime, D_e and D_x are the respective electron and exciton generation rates.

The two equations in system (1) are closed by the following boundary conditions:

- **Initial conditions:**

$$\left[\begin{array}{l} D_e \dfrac{dn_e}{dz} = S_e(n_e - n_{e0}) \\ D_x \dfrac{dn_x}{dz} = S_x(n_x - n_{x0}) \end{array} \right]_{z=0} \quad (2)$$

➢ **Final conditions:**

$$\begin{cases} D_e \dfrac{dn_e}{dz} = -S_e(n_e - n_{e0}) \\ D_x \dfrac{dn_x}{dz} = -S_x(n_x - n_{x0}) \end{cases}_{z = L_p} \quad (3)$$

Where S_e and S_x represent the electron and exciton recombination velocities, respectively.

3.2. Electron transport equations and adimensional boundary conditions:

To facilitate the numerical solution of these equations, it is often necessary to dimensionalize them in order to have homogeneous solutions.

By positing $z = z^*L$, $w = w^*L$, $n_e = n_e^* N_r$, and $n_x = n_x^* N_r$ and replacing z, w, n_e and n_x with their values in the systems of equations (1), one obtains the following dimensionless diffusion equations.

$$\begin{cases} F_{0e} \dfrac{\partial^2 n_e^*}{\partial z^{*2}} + K_e \dfrac{\partial n_e^*(w_p^* - z^*)}{\partial z^*} = -A_e(n_x^* - n_{x0}^*) + B_e(n_e^* - n_{e0}^*) + (n_e^* - n_{e0}^*) - G_e^* \\ F_{0x} \dfrac{\partial^2 n_x^*}{\partial z^{*2}} + K_x \dfrac{\partial n_x^*(w_p^* - z^*)}{\partial z^*} = A_x(n_x^* - n_{x0}^*) - B_x(n_e^* - n_{e0}^*) + (n_x^* - n_{x0}^*) - G_x^* \end{cases} \quad (4)$$

With:

$$F_{0e} = \frac{D_e \tau_e}{L^2} \qquad K_e = \mu_e \tau_e \frac{E_0}{w} \qquad A_e = \frac{\tau_e}{\tau_d} \qquad B_e = b\tau_e N_A \qquad G_e^* = \frac{8}{9}\frac{\tau_e}{N_r} G$$

$$F_{0x} = \frac{D_x \tau_a}{L^2} \qquad K_x = \mu_x \tau_a \frac{E_0}{w} \qquad A_x = \frac{\tau_a}{\tau_d} \qquad B_x = b\tau_a N_A \qquad G_x^* = \frac{1}{9}\frac{\tau_a}{N_r} G$$

By proceeding in the same way, we obtain the dimensionless boundary conditions.

➢ **Initial conditions:**

$$\begin{cases} A_{de} \dfrac{dn_e^*}{dz^*} = (n_e^* - n_{e0}^*) \\ A_{dx} \dfrac{dn_x^*}{dz^*} = (n_x^* - n_{x0}^*) \end{cases}_{z^* = 0} \quad (5)$$

➢ **Final conditions:**

$$\begin{cases} A_{Le} \dfrac{dn_e^*}{dz^*} = -(n_e^* - n_{e0}^*) \\ A_{Lx} \dfrac{dn_x^*}{dz^*} = -(n_x^* - n_{x0}^*) \end{cases}_{z^* = L_p^*} \quad (6)$$

With:

$$A_{de} = A_{Le} = \frac{D_e}{S_e L} \qquad A_{dx} = A_{Lx} = \frac{D_x}{S_x L}$$

Some parameters such as the scattering coefficients of holes, electrons and excitons of these equations depend on the temperature. The equations being non-linear, the calculation does not have an analytical solution and must be self-consistent. Therefore, a numerical solution of these equations is necessary.

3.3 Numerical (algebraic) model of the continuity equations in the base:

To obtain a numerical solution of our problem, we must transform the differential equations of the mathematical model into a system of algebraic equations obtained after discretization. We have chosen the power law as a discretization method. This method consists in integrating the equations on a discrete set called control volume. This results in the system of algebraic equations (7).

$$\begin{cases} b_{1,k}.n_{k,I_0} - c_{1,k}.n_{k,I_0+1} = d_{1,k} & i = I_0 \\ -a_{w,k}.n_{k,i-1} + a_{M,k}.n_{k,i} - a_{r,k}.n_{k,i+1} = S_{m,k} & I_0 + 1 \leq i \leq I_m - 1 \\ -a_{m,k}.n_{k,I_m-1} + b_{m,k}.n_{k,I_m} = d_{m,k} & i = I_m \end{cases} \quad (7)$$

With here:

$$b_{1,k} = a_{M1,k} - 2.C_{dk}.a_{w1,k} \quad ; \quad c_{1,k} = a_{r1,k} - a_{w1,k} \quad ; \quad d_{1,k} = s_{1,k} - 2.C_{dk}.a_{w1,k}.n_{k0}$$

$$C_{Lk} = \frac{\delta z_{I_m}}{A_{Lk}} \quad ; \quad a_{m,k} = 1 \quad ; \quad b_{m,k} = 1 + C_{Lk} \quad ; \quad d_{m,k} = C_{Lk}n_{k0}$$

The coefficients $a_{w,k}$, $a_{M,k}$ and $a_{r,k}$ are evaluated at the interfaces of the control volume using the power law scheme. They represent the combined conduction and diffusion fluxes. The expressions for these coefficients are given in [39].

With the coefficients of the discrete equations represented in the following table.

Table1: Expressions of the coefficients of linear systems

Coefficients	Expressions
$a_{w,k}$	$D_{w,k}.A(P_{w,k}) + Max[F_{w,k}; 0]$
$a_{M,k}$	$a_{r,k} + a_{w,k} + S_{M,k}$
$a_{r,k}$	$D_{r,k}.A(P_{r,k}) + Max[-F_{r,k}; 0]$

The obtained system being strongly non-linear, the use of an iterative method is necessary.

3.4. Ancillary calculations of the numerical program:

3.4.1. Carrier photo-current density:

The photocurrent density is composed of the scattering current due to carrier scattering via photons and the conduction current due to the effect of the electric field of the space charge region.

3.4.2. Conduction current:

In a material, charged electrons collide with atoms in the crystal lattice. Each shock corresponds to a loss of energy. Between two shocks, the electrons are accelerated uniformly in the opposite direction of the electric field E(z) of the ECZ with a velocity $\vartheta(z) = \mp\mu.E(z)$. The photocurrent density is then written:

- **For electrons:**

$$J_{c,e} = q.n_e.m_e.E(z) \quad (8)$$

- **For excitons:**

$$J_{c,x} = q.n_x.m_x.E(z) \quad (9)$$

The velocities $\vartheta_e(z)$ and $\vartheta_x(z)$ are proportional to the electric field. The sign of the carrier mobility coefficients $\mu_e(z)$ and $\mu_x(z)$ depends on their charges (-q).

3.4.3. Diffusion current:

Fick's law, which is an experimental law established in by Adolphe Fick, states that: the number of particles per unit time and volume (Φ) is defined by the equation $(\Phi) = -D\frac{dn}{dz}$ [40].

From this expression, we can deduce, the photocurrent densities of electrons and excitons.

- **For electrons:**

$$J_{d,e} = q.D_e.\frac{dn_e}{dz} \quad (10)$$

- **For excitons:**

$$J_{d,x} = q.D_x.\frac{dn_x}{dz} \quad (11)$$

3.4.4. Photocurrent densities of charge carriers:

The photocurrent densities of electrons and excitons are the sums of the two contributions: the diffusion and the conduction currents.

- **For electrons:**

$$J_e = q.n_e.m_e.E(z) + q.D_e.\frac{dn_e}{dz} \quad (12)$$

- **For excitons:**

$$J_x = q.n_x.m_x.E(z) + q.D_x.\frac{dn_x}{dz} \quad (13)$$

The resultant of the photocurrent densities of the electrons and excitons is the total photocurrent density of the carriers in the $J = J_e + J_x$ basis.

3.4.5. Spectral response and quantum efficiency:

The spectral response (SR) is, analogously, the ratio of the intensity $I(\lambda)$ generated by the cell to the incident power $P_0(\lambda)$, for each wavelength. It is thus to illuminate the cell and measure the current it delivers.

$$SR(l) = \frac{I(l)}{P_0(l)} = \frac{I(l)/S}{j_0(l)} = \frac{J(l)}{j_0(l)} \quad (14)$$

Where $\varphi_0(\lambda)$ is the incident photon flux and S is the area of the cell. To calculate the absorbed photon flux, we make the difference between the photon flux at the entrance of the material (the illuminated face) and the photon flux transmitted at a depth z in the base. It then comes:

$$j_a(l) = j_0(l)[1- R(l)][1- e^{a(l).z}] \quad (15)$$

It is generally this quantity which is measured and which makes it possible to calculate the quantum efficiency.

We distinguish the external quantum efficiency (EQE) of internal quantum efficiency (IQE) in which we take into account the flow of photons absorbed by the active layer of the cell.

$$EQE(l) = \frac{J(l)}{q.l.j_0(l)} \quad (16)$$

The expression presented here takes into account optical losses such as reflection or transmission through the cell: it is the external quantum efficiency.

It can be corrected for optical losses to give the IQE which takes into account the characteristics of the cell (scattering, surface and volume recombinations and / or absorption of the material considered).

By definition, the IQE is the ratio between the number of photons transmitted and photogenerated on the number of photons absorbed. It can also be defined as the ratio between the EQE and the absorption coefficient of the layer of thickness z.

$$IQE(l) = \frac{EQE(l)}{A(l)} \quad (17)$$

With here: $A(\lambda) = [1 - R(\lambda)][1 - e^{\alpha(\lambda).z}]$ being the absorption coefficient of the layer of thickness z. The results from this program or calculation code are discussed and interpreted.

4. Results and discussion

Since the dependence of the kinematic and intrinsic parameters and especially the charge carrier behavior in the silicon heterojunction photovoltaic cell is still under discussion, we are interested in the effect of the exciton annihilation lifetime with respect to some kinematic and intrinsic parameters, with emphasis on their dependencies. Thus, exciton annihilation is a function of temperature and doping rate in the base (N_A). The cell is overdoped in donor atom on one hand (emitter) and doped in acceptor atom on the other hand (base), so we can consider that the doping rate is constant and remains fixed once the majority carrier balance between emitter and base is established and the space charge region is created.

Therefore, the effect of temperature on the exciton annihilation lifetime is studied by varying the doping rate in the base to have the most suitable value so that excitons cannot harm the cell energy production (HIT).

4.1 Choice of doping rate:

In Figure 4 is plotted the annihilation lifetime as a function of temperature with different values of the doping rate (N_A).

At low temperatures (below 273 K), regardless of the doping rate, used here, the exciton annihilation lifetimes remain low in the vicinity of $1x10^{-5}$ s. Above 273 K, we observe an increase in the exciton

annihilation lifetime that reaches $7.298x10^{-5}$ s for a doping rate of $1.12x10^{17}$ cm^{-3}, $3.901x10^{-5}$ s for a spiking rate of $1.13x10^{17}$ cm^{-3} and $5.825x10^{-6}$ s for a spiking rate of $1.14x10^{17}$ cm^{-3}.

We can see that increasing the temperature is favorable for the time at which excitons annihilate. On the other hand, an increase in doping significantly decreases the time taken by the exciton in the semiconductor before annihilating.

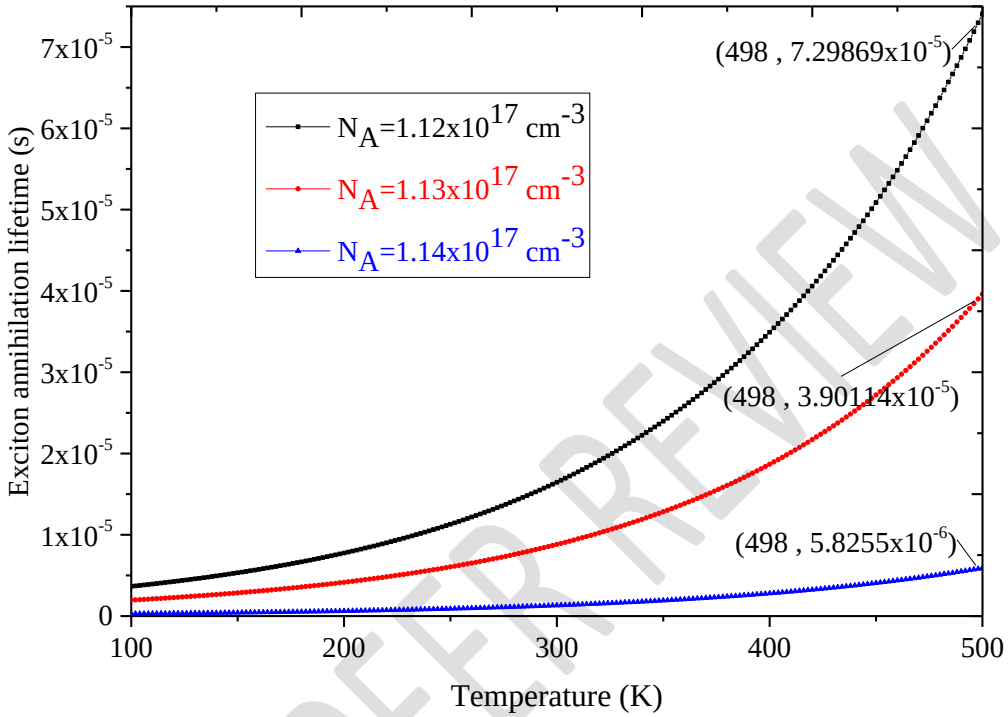

Figure 4: Exciton annihilation lifetime as a function of temperature with different values of the doping rate

The excitatory effect of the temperature defined in [41] allows the excitons to last before annihilating. On the other hand, increasing the doping rate creates recombination sites or defects which decrease the time taken by the excitons before annihilation.

For consistency and physical reality, we decided to set the doping rate ($N_A = 1.14x10^{17}$ cm^{-3}). With this value, we obtain annihilation lifetimes close to and less than or equal to the electron lifetimes. This is logical, because excitons do not often last in the cell.

After having chosen the doping rate to have adequate annihilation lifetimes and to have evaluated the effect of an external parameter (temperature) on the annihilation lifetime to better understand the physical phenomena, we will study the diffusion lengths of electrons and excitons as a function of the annihilation lifetime of excitons.

4.2 Scattering length of charge carriers

Figures 5 and 6 represent respectively the scattering lengths of electrons and excitons at the same scale and at different scales as a function of the annihilation lifetime of excitons.

We can see from Figure 5 that electrons scatter the farthest than excitons and the scattering length of excitons increases from a value of 0.00262 cm to a value of 0.02307 cm, when the exciton annihilation lifetime is increased from a value of $3.06797x10^{-7}$ s to a value of $5.91366x10^{-6}$ s.

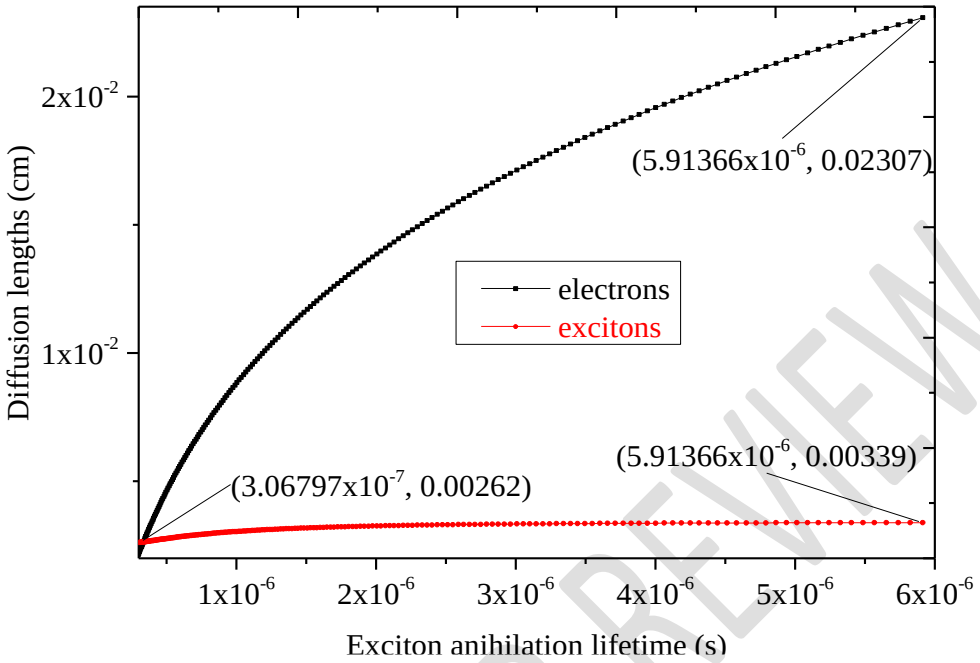

Figure 5: Scattering lengths of electrons and excitons as a function of the exciton annihilation lifetime

Since the excitonic physical quantities are small when compared to the physical quantities of the free electron-hole pairs, we have in figure 6 a growth of the scattering lengths of free electrons and excitons from a value of 0.00262 cm to a value of 0.00339 cm, for exciton annihilation lifetimes ranging from $3.06797x10^{-7}$ s to $5.91366x10^{-6}$ s.

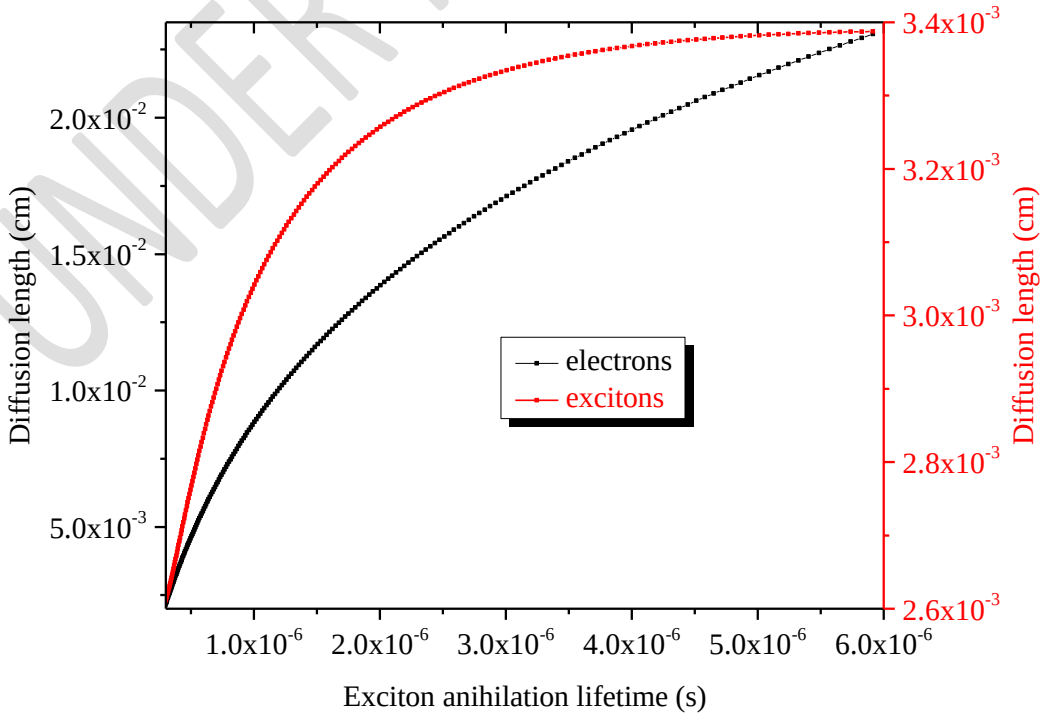

Figure 6: Scattering lengths of electrons and excitons at different scales as a function of the annihilation lifetime of excitons

The excitons spending more time in the photovoltaic cell before being annihilated diffuse as far as possible thanks to the excitation energy which, in the form of kinetic energy, diffuses them until they annihilate.

In the case of free electron scattering, the annihilation lifetime of the excitons is affected by the temperature effect. By delaying the annihilation of excitons, we bring a stability of the free charge carriers for a certain time, which allows the electrons to diffuse as far as possible. In addition, the annihilation of excitons in a delocalised state creates excitons with energy levels greater than or equal to their energies before they annihilate, allowing the excitons to diffuse as far as possible. So, everything that delays the annihilation process is favorable to the diffusion of charge carriers.

4.3. Density of charge carriers

Figures 7 and 8 represent respectively the electron and exciton densities as a function of the depth of crystalline silicon with different values of the exciton annihilation lifetime.

An increase in the exciton annihilation lifetime leads to a decrease in the electron density and an increase in the exciton density.

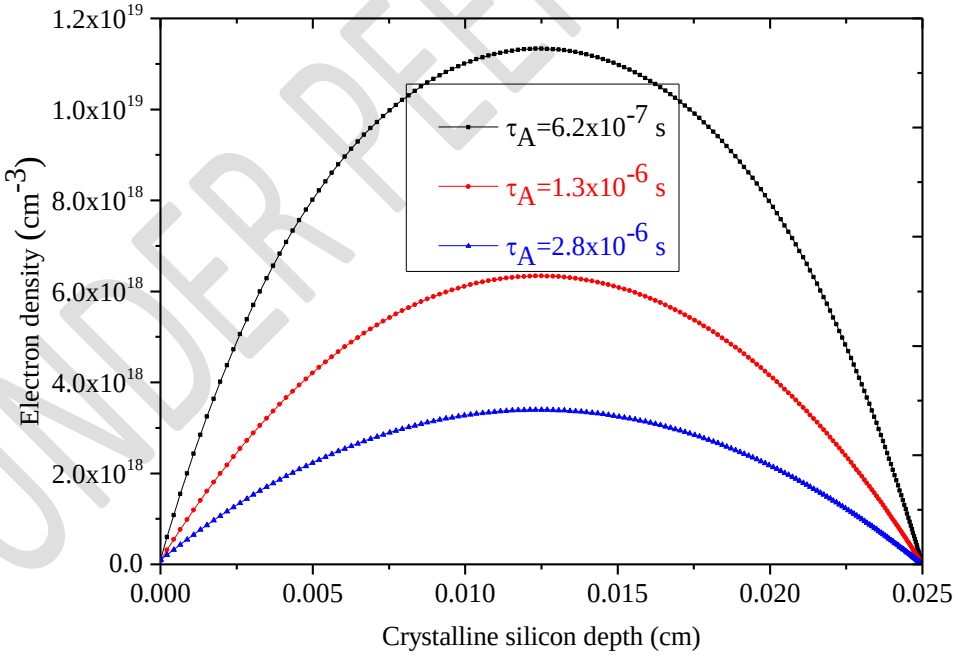

Figure 7: Electron density as a function of depth in crystalline silicon with different values of exciton annihilation lifetime.

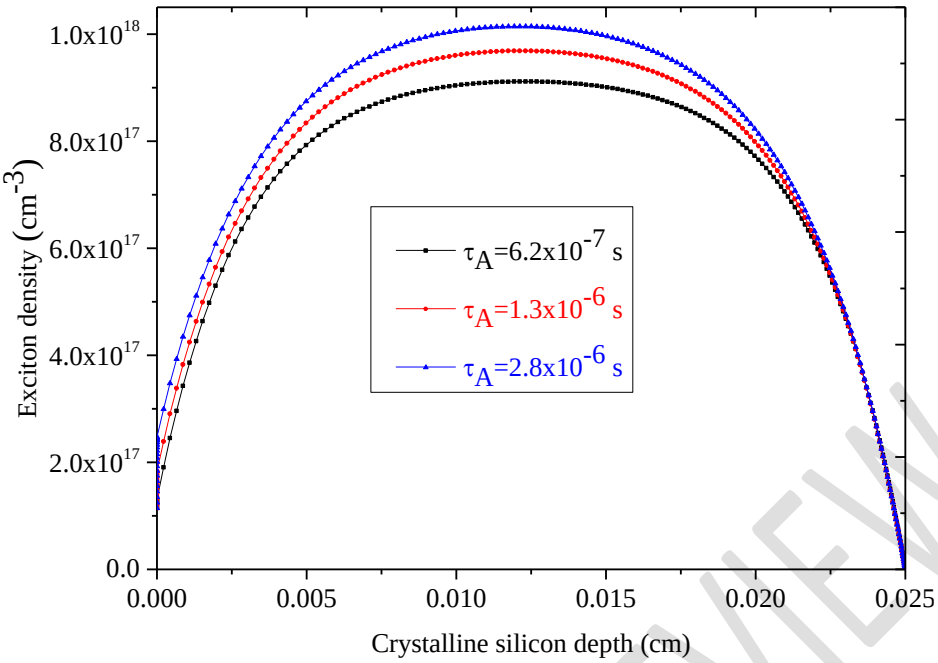

Figure 8: Density of excitons as a function of the depth of the crystalline silicon with different values of the annihilation lifetime of excitons

As the annihilation lifetime of the excitons increases, their numbers in the cell increase due to the loss of energy of the free electrons which relax to occupy excited levels. These relaxation phenomena combined with direct recombinations decrease the density of free electrons. Hence the antagonistic effect on the mobility of charge carriers described in [30], which is manifested with the annihilation lifetime of excitons. Furthermore, we can say that the fact that excitons do not last in the photovoltaic cell is favorable to the density of free electrons.

To produce electricity from photovoltaic origin, it is important to have a large amount of charge carriers in the cell, but it is more useful to direct and diffuse them to the collectors, so that they can be collected and participate in the electrical charges.

However, the ordered movement of the charge carriers towards the receiving electrodes is the photocurrent density of the charge carriers. These will be studied as a function of the annihilation lifetime, to better understand the excitonic phenomena in the cell.

4.4. Photocurrent density of load carriers

Figure 9 shows the photocurrent densities of electrons, excitons and total as a function of the annihilation life of excitons. The photocurrent densities of electrons and total increase with the annihilation life, while the photocurrent density of excitons decreases.

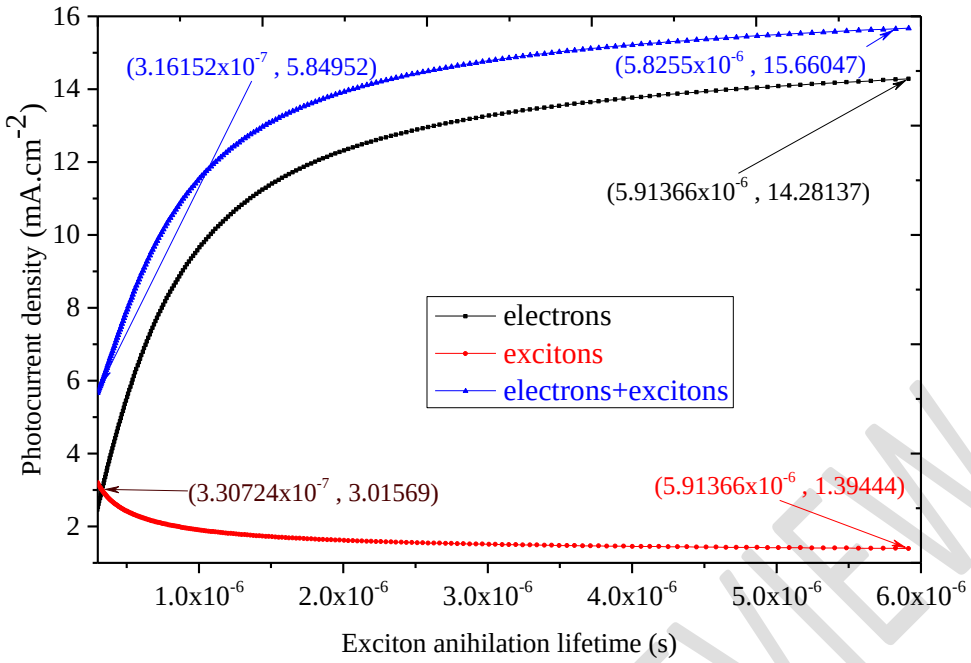

Figure 9: Photocurrent density of charge carriers as a function of exciton annihilation lifetime.

Delayed annihilation of excitons when they are generated in the cell often leads to energy losses by direct recombination, which can reduce the photocurrent density of excitons that are in an unstable state.

On the other hand, by increasing the life time of the exciton before its annihilation, one decreases the phenomena of relaxation and radiative recombination which decreases the generation of free charge carriers. Thus, it is more cost effective to have higher annihilation lifetimes to have the maximum number of photons generated by free carriers, than to use low annihilation lifetimes to have a minimal contribution of bound electrons, as free charge carriers are in the majority in the cell and generate the largest number of photons.

To better understand the participation of charge carriers when the exciton annihilation lifetime is varied, we will make a study of the internal quantum efficiency of electrons, excitons and total.

4.5. The internal quantum efficiency of charge carriers

In terms of efficiency, we get a clear picture of the participation of each of the two types of charge carriers shown in Figure 10.

Specifically, we observe internal quantum efficiency ranging from 14.98221%, for an exciton annihilation lifetime of $3.25793x10^{-7}$ s to respective values of internal quantum efficiency of free electrons and excitons of 70.92697% and 6.92534%, for an exciton annihilation lifetime of $5.91366x10^{-6}$ s.

This, for the same exciton annihilation lifetimes, leads to internal quantum efficiency of the HIT cell between 29.29768% and 77.8525%.

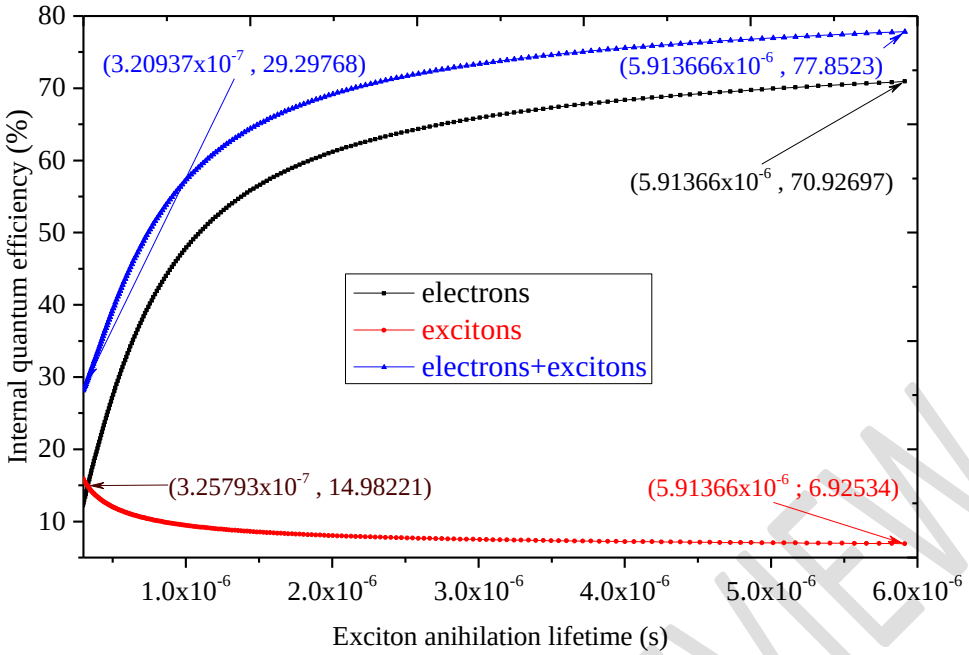

Figure 10: Internal quantum efficiency of charge carriers as a function of the annihilation lifetime of excitons

When excitons are annihilated, they remain bound at different energy levels, which makes it difficult to dissociate them. For them to contribute to quantum efficiency, they have to be dissociated. Hence a decrease in the internal quantum yield of excitons as a function of their annihilation lifetime.

On the other hand, when excitons annihilate, they create new charge carriers in the cell by multiphonon relaxation, leading to a surplus of free charge carriers. So, the longer excitons remain in the cell without being annihilated, the fewer free electrons recombine and the greater their contribution to HIT cell yield.

5. Conclusion

After evaluating the doping rates as a function of the annihilation lifetime, we found a value for the doping rate (A). With this value, we obtained annihilation lifetimes close to A and less than or equal to the electron lifetime. This is logical, as excitons do not often last in the cell and their lifetime is shorter than the lifetime of electrons.

Secondly, excitons scatter as far as possible thanks to their excitation energy. Whereas free electrons diffuse as far as possible thanks to the stability of the free charge carriers over a certain period of time, due to a reduction in the annihilation lifetime of the excitons that occurs through the effect of temperature. So, anything that delays the exciton annihilation process is conducive to charge carrier diffusion.

In addition to charge carrier diffusion, relaxation phenomena combined with direct recombination, which occur during exciton annihilation, reduce the density of free electrons. Furthermore, we can say that the fact that the excitons do not exist in the photovoltaic cell is favourable to the density of free

electrons. The ordered movement of these towards the receiving electrodes is the photocurrent density of the charge carriers.

Finally, it is more profitable to have higher annihilation lifetimes in order to have the maximum number of photons generated by free carriers, than to use low annihilation lifetimes to have a minimal contribution from bound electrons, because free charge carriers are in the majority in the cell and generate the greatest number of photons. The profitability of the photons generated is well evaluated by the cell's internal quantum yields, which range from 29.29768% to 77.8525%.

Disclaimer (Artificial intelligence)

Option 1:

Author(s) hereby declare that NO generative AI technologies such as Large Language Models (ChatGPT, COPILOT, etc) and text-to-image generators have been used during writing or editing of manuscripts.

Option 2:

Author(s) hereby declare that generative AI technologies such as Large Language Models, etc have been used during writing or editing of manuscripts. This explanation will include the name, version, model, and source of the generative AI technology and as well as all input prompts provided to the generative AI technology

Details of the AI usage are given below:

1.

2.

3.

Références :

[1]. R. Corkish, D. S. P. Chan and M. A. Green ; Excitons in silicon diodes and solar cells: A three-particle theory ; Institute of Physics, 1996, 79(1), pp 195-203.

[2]. A. Hangleiter ; Nonradiative recombination via deep impurity levels in silicon: Experience ; Physical Review B, 1987, 35(17), pp 9149-9161.

[3]. A. Hangleiter ; Nonradiative recombination via deep impurity levels in semiconductors: The Auger Excitonic Mechanism ; Physical Review B, 1988, 37(5), pp 2594-2604.

[4]. A. Hangleiter and R. Hacker ; Enhancement of band-to-band Auger recombination by electron-hole correlations ; Phys. Rev. Lett, 1990, 65(2), pp 215-218.

[5]. J. P. Wolfe and A. Mysyrowicz ; Excitonic matter ; Scientific American, 1984, 250(3), pp 70-79.

[6]. J. Dziewior and W. Schmidt ; Auger coefficients for highly doped and highly excited silicon ; Applied Physics Letters, 1977, 31(5), pp 346-348.

[7]. M. Faye, M. Mbow et M. Ba ; Numerical modeling of the effects of excitons in solar cell junction n^+p of the model by extended the space charge layer ; International Review of Physics ; 2014, 8(4), pp.102-109

[8]. M. Balkanski, État actuel du problème de l'exciton, J. Phys. Radium, 1958, 19 (2), pp.170-182.

[9]. G. Soavi, S. D. Conte, C. Manzoni, D. Viola, A. Narita, Y. Hu, X. Feng, U. Hohenester, E. Molinari, D. Prezzi, K. Müllen and G. Cerullo ; Exciton–exciton annihilation and biexciton stimulated emission in graphene nanoribbons ; Nature Communications, 2016, 7(11010) ; pp 1-7.

[10]. J. Fiuràšek, Engineering quantum operations on traveling light beams by multiple photon addition and subtraction, Phys. Rev. A 80 [quant-ph], 2009, 80(5), pp 1-7.

[11]. May, V. (2014). Kinetic theory of exciton–exciton annihilation. The Journal of Chemical Physics, 140(5), 054103.

[12]. Peng, W., Rupich, S. M., Shafiq, N., Gartstein, Y. N., Malko, A. V., & Chabal, Y. J. (2015). Silicon Surface Modification and Characterization for Emergent Photovoltaic Applications Based on Energy Transfer. Chemical Reviews, 115(23), 12764–12796.

[13]. Yeltik, A., Guzelturk, B., Hernandez-Martinez, P. L., Govorov, A. O., & Demir, H. V. (2013). Phonon-Assisted Exciton Transfer into Silicon Using Nanoemitters: The Role of Phonons and Temperature Effects in Förster Resonance Energy Transfer. ACS Nano, 7(12), 10492–10501.

[14]. Chen, J., Schmitz, A., Inerbaev, T., Meng, Q., Kilina, S., Tretiak, S., & Kilin, D. S. (2013). First-Principles Study of p-n-Doped Silicon Quantum Dots: Charge Transfer, Energy Dissipation, and Time-Resolved Emission. The Journal of Physical Chemistry Letters, 4(17), 2906–2913.

[15]. Xia, P., Raulerson, E. K., Coleman, D., Gerke, C. S., Mangolini, L., Tang, M. L., & Roberts, S. T. (2019). Achieving spin-triplet exciton transfer between silicon and molecular acceptors for photon upconversion. Nature Chemistry.

[16]. Yuan, L., & Huang, L. (2015). Exciton dynamics and annihilation in WS2 2D semiconductors. Nanoscale, 7(16), 7402–7408.

[17]. Linardy, E., Yadav, D., Vella, D., Verzhbitskiy, I. A., Watanabe, K., Taniguchi, T., … Eda, G. (2020). Harnessing exciton-exciton annihilation in two-dimensional semiconductors. Nano Letters.

[18]. Sortino, L., Gülmüs, M., Tilmann, B. et al. Radiative suppression of exciton–exciton annihilation in a two-dimensional semiconductor. Light Sci Appl **12**, 202 (2023).

[19]. Le LV, Huong TTT, Nguyen T-T, Nguyen XA, Nguyen TH, Cho S, Kim YD, Kim TJ. The Wannier-Mott Exciton, Bound Exciton, and Optical Phonon Replicas of Single-Crystal GaSe. *Crystals*. 2024; 14(6):539.

[20]. Postorino S, Sun J, Fiedler S, Lee Cheong Lem LO, Palummo M, Camilli L. Interlayer Bound Wannier Excitons in Germanium Sulfide. *Materials*. 2020; 13(16):3568.

[21]. Poszwa, A. Geometry-modulated dipole polarizability of the two-dimensional Mott-Wannier excitons in gate-defined anisotropic quantum dot. Sci Rep **12**, 14774 (2022).

[22]. Gillett, A.J., Privitera, A., Dilmurat, R. et al. The role of charge recombination to triplet excitons in organic solar cells. Nature **597**, 666–671 (2021).

[23]. Zeiske, S., Sandberg, O.J., Zarrabi, N. et al. Direct observation of trap-assisted recombination in organic photovoltaic devices. Nat Commun **12**, 3603 (2021).

[24]. Chen, P., Atallah, T.L., Lin, Z. et al. Approaching the intrinsic exciton physics limit in two-dimensional semiconductor diodes. Nature **599**, 404–410 (2021).

[25]. Brem, S., Selig, M., Berghaeuser, G., & Malic, E. (2018). Exciton Relaxation Cascade in two-dimensional Transition Metal Dichalcogenides. Scientific Reports, 8(1).

[26]. Kambhampati, P. (2011). Hot Exciton Relaxation Dynamics in Semiconductor Quantum Dots: Radiationless Transitions on the Nanoscale. The Journal of Physical Chemistry C, 115(45), 22089–22109.

[27]. Jumper, C. C., Anna, J. M., Stradomska, A., Schins, J., Myahkostupov, M., Prusakova, V., … Scholes, G. D. (2014). Intramolecular radiationless transitions dominate exciton relaxation dynamics. Chemical Physics Letters, 599, 23–33.

[28]. Yu, J., Lammi, R., Gesquiere, A. J., & Barbara, P. F. (2005). Singlet−Triplet and Triplet−Triplet Interactions in Conjugated Polymer Single Molecules. The Journal of Physical Chemistry B, 109(20), 10025–10034.

[29]. King, S. M., Dai, D., Rothe, C., & Monkman, A. P. (2007). Exciton annihilation in a polyfluorene: Low threshold for singlet-singlet annihilation and the absence of singlet-triplet annihilation. Physical Review B, 76(8).

[30]. O. Ngom, M. Faye, S. Ndiaye, C. Mbow, B. Ba ; Behavior of free electrons and excitons, due to their mobility under the effects of optoelectric parameters in a silicon heterojunction cell (HIT) : Interdependence of physical phenomena acting on free and bound load carriers ; Journal of Scientific and Engineering Research, 2020, 7(5) ; pp 1-15.

[31]. G. Sahin, M. Dieng, M. A. Ould El Moujtaba, M. I. Ngom, A. Thiam, G. Sissoko ; Capacitance of Vertical Parallel Junction Silicon Solar Cell under Monochromatic Modulated Illumination ; Journal of Applied Mathematics and Physics, 2015, 3(11) ; pp 1536-1543.

[32]. S. Mbodji, M. Zoungrana, I. Zerbo, B. Dieng, G. Sissoko ; Modelling Study of Magnetic Field's Effects on Solar Cell's Transient Decay ; World Journal of Condensed Matter Physics, 2015, 5 ; pp 284-293.

[33]. B.H. Rose and H.T. Weaver, Determination of Effective Surface Recombination Velocity and Minority Carrier Lifetime in High-Efficiency Si Solar Cells, Journal of Applied Physics, 1983, 54(1), pp 238-247.

[34]. M. Faye, M. MBow, M. Ba ; Numerical Modeling of the Effects of Excitons in a Solar Cell Junction n+p of the Model by Extending the Space Charge Layer ; International Review of Physics (I.RE.PHY) ; 8(4), ISSN 1971-680X (August 2014).

[35]. S. Zh. Karazhanov, Temperature and doping level dependence solar cell performance Including excitons, Solar Energy Materials & Solar Cells 63 (2000), pp 149-163.

[36]. R. Corkish, D. S. P. Chan, and M. A. Green ; Excitons in silicon diodes and solar cells: A three-particle theory, Institute of Physics. [(S0021-8979(1996) 0070-9].

[37]. J. Aberg, Catalytic Coherence, Phys. Rev. Lett. 113 [quant-ph], Vol. 3, 2014, pp 1-39.

[38]. J. Vogel, W. Li, A. Mokhberi, I. Lesanovsky, and F. Schmidt-Kaler ; Shuttling of Rydberg ions for fast entangling operations ; Phys. Rev. Lett. 123 [physics.atom-ph] ; Vol. 2, 2019 ; pp 1-8.

[39]. A. Hangleiter and R. Hacker ; Enhancement of band-to-band Auger recombination by electron-hole correlations ; Phys. Rev. Lett, 1990, 65(2), pp 215-218.

[40]. C. Truesdell ; Mechanical Basis of Diffusion ; The Journal of Chemical Physics, 1962, 37(10), pp 2336–2344.

[41]. O. Ngom, M. Faye, M. Mbaye, C. Mbow and B. Ba ; Numerical Study of the Effect of Temperature on the Performance of a Silicon Heterojunction Solar Cell (HIT) in the Presence of Excitons ; International Journal of Materials Science and Applications, Special Issue : Advanced Materials for Energy Storage and Conversion Applications, 8(4), pp 56-67.